Micro- and nanoelectronics. Condensed matter physics

Микро- и наноэлектроника. Физика конденсированного состояния

UDC 621.382
https://doi.org/10.32362/2500-316X-2025-13-6-86-94
EDN KOATTE

RESEARCH ARTICLE

Interface traps build-up and its influence on electrostatic discharge robustness of high-power metal-oxide-semiconductor field-effect transistor

Diana M. Bakerenkova [@], **Aleksandr S. Petrov**

Research Institute of Scientific Instruments, Lytkarino, 140080 Russia
[@] *Corresponding author, e-mail: arzamasceva.diana@mail.ru*

• **Submitted:** 16.05.2025 • **Revised:** 24.06.2025 • **Accepted:** 06.10.2025

Abstract

Objectives. The aim of the study is to confirm that the robustness of high-power metal–oxide–semiconductor field-effect transistor (MOSFET) to electrostatic discharge (ESD) after gamma irradiation is determined by the concentration of built-up interface traps (IT). The reason for such dependence is the degradation of the gain of the parasitic bipolar transistor in the structure of high-power MOSFETs during accumulation of IT. As a result, higher ESD pulse voltage is required to activate the parasitic bipolar transistor and cause the subsequent catastrophic failure of MOSFET.

Methods. The study describes the physical mechanism of the influence of IT accumulation on the robustness of high-power MOSFETs to ESD. Experimental studies included determination of ESD robustness for two types of high-power MOSFETs before irradiation, ^{60}Co gamma irradiation to several levels of total ionizing dose, and subsequent determination of the ESD robustness of irradiated samples.

Results. The study developed a method for calculating IT concentration and radiation-induced charge density from subthreshold drain-gate characteristics. It was also shown that for the first type of MOSFET, when irradiated to total ionizing dose level of 3 krad, the build-up IT did not occur, nor was any change or insignificant decrease in the breakdown voltage observed when exposed to ESD. For the second type of MOSFET, build-up IT was observed when irradiated to total ionizing dose level of 2 and 4 krad and an increase in the breakdown voltage was also observed when exposed to ESD.

Conclusions. The study shows the relationship between the IT concentration and the change in the breakdown voltage when exposed to ESD. The results obtained can be used to assess the failure-free operation time of devices operating under conditions of ionizing radiation and electrostatic discharges.

Keywords: electrostatic discharge, radiation effects, interface traps, high-power MOSFETs

For citation: Bakerenkova D.M., Petrov A.S. Interface traps build-up and its influence on electrostatic discharge robustness of high-power metal-oxide-semiconductor field-effect transistor. *Russian Technological Journal.* 2025;13(6):86–94. https://doi.org/10.32362/2500-316X-2025-13-6-86-94, https://www.elibrary.ru/KOATTE

Financial disclosure: The authors have no financial or proprietary interest in any material or method mentioned.

The authors declare no conflicts of interest.

НАУЧНАЯ СТАТЬЯ

Влияние встраивания поверхностных состояний на стойкость мощных металлооксидных полупроводниковых полевых транзисторов к электростатическому разряду

Д.М. Бакеренкова [@], **А.С. Петров**

АО «Научно-исследовательский институт приборов», Лыткарино, 140080 Россия
[@] *Автор для переписки, e-mail: arzamasceva.diana@mail.ru*

• **Поступила:** 16.05.2025 • **Доработана:** 24.06.2025 • **Принята к опубликованию:** 06.10.2025

Резюме

Цели. Целью исследования является проверка гипотезы о том, что стойкость мощных металлооксидных полупроводниковых полевых транзисторов (МОПТ) к электростатическому разряду (ЭСР) после гамма-облучения определяется концентрацией встроившихся в процессе облучения поверхностных состояний (ПС). Причиной такой зависимости является деградация коэффициента усиления паразитного биполярного транзистора в структуре мощных МОПТ при накоплении ПС. Как следствие, для включения паразитного биполярного транзистора и последующего выхода из строя МОПТ требуется все большее напряжение импульса ЭСР.

Методы. Теоретическое описание физического механизма накопления ПС и его влияния на стойкость мощных МОПТ к ЭСР. Экспериментальные исследования, включающие определение стойкости к ЭСР двух типов необлученных МОПТ с помощью специально разработанного генератора ЭСР, облучение гамма-квантами ^{60}Co в активном электрическом режиме до нескольких уровней поглощенной дозы и последующее определение стойкости облученных образцов к ЭСР.

Результаты. Разработан метод, позволяющий численно рассчитать зависимости тока стока от напряжения затвор-исток для любых значений плотности накопленного радиационно-индуцированного заряда и концентрации встроившихся ПС. Показано, что для 1-го типа МОПТ при облучении до уровня поглощенной дозы в 3 крад встраивание ПС не происходило, и также не наблюдалось изменение пробивного напряжения при воздействии ЭСР или наблюдалось его незначительное снижение. Для 2-го типа МОПТ наблюдалось встраивание ПС при облучении до уровня поглощенной дозы в 2 и 4 крад, а также увеличение пробивного напряжения при воздействии ЭСР.

Выводы. Показана связь между концентрацией встроившихся ПС и изменением стойкости мощных МОПТ к ЭСР. Полученные результаты могут быть использованы при оценке времени безотказной работы устройств, работающих в условиях одновременного воздействия радиационных и импульсных электрических нагрузок.

Ключевые слова: электростатический разряд, радиационные эффекты, поверхностные состояния, мощные МОП-транзисторы

Для цитирования: Бакеренкова Д.М., Петров А.С. Влияние встраивания поверхностных состояний на стойкость мощных металлооксидных полупроводниковых полевых транзисторов к электростатическому разряду. *Russian Technological Journal*. 2025;13(6):86–94. https://doi.org/10.32362/2500-316X-2025-13-6-86-94, https://www.elibrary.ru/KOATTE

Прозрачность финансовой деятельности: Авторы не имеют финансовой заинтересованности в представленных материалах или методах.

Авторы заявляют об отсутствии конфликта интересов.

Glossary

Electrostatic discharge is a pulse transfer of the electrostatic charge between bodies with different electrostatic potentials.

Total ionizing dose is the amount of ionizing radiation energy absorbed by a substance per unit mass.

Total ionizing dose effects are effects caused by the loss of energy in a substance due to ionizing radiation for ionization.

Secondary breakdown is a sharp drop in collector-emitter voltage caused by thermal instability or avalanche injection.

Interface traps are energy states (energy levels) of conduction electrons localized near the surface of a solid.

Displacement damage is effect caused by the loss of energy due to ionizing radiation in a substance, resulting in structural damage.

Space charge region is an electrically charged layer which forms at the boundary between *n*- and *p*-areas.

Radiation-induced charge is a positive charge which accumulates in the gate dielectric of transistors under the influence of ionizing radiation.

INTRODUCTION

Research into the effect of radiation loads upon the breakdown voltage of *p-n* junctions has relatively recently been actively resumed [1–3]. Previously no critical change in the breakdown voltage of *p-n* junctions was observed after radiation exposure up to an total ionizing dose (TID) dose $4 \cdot 10^4$ rad(Si) [4, 5]. However, when a static or linearly increasing voltage is applied, the effect of electrostatic discharges (ESD) and the subsequent breakdown of *p-n* junctions manifest themselves through a more complex mechanism than breakdown.

One of the first works on this topic was published in 2017 [6] and it examines the influence of dose effects on ESD protection devices: P+/NW-diodes, Zener diodes, and gate-grounded *n*-type metal-oxide semiconductor (GGNMOS) transistors. Helium ions with an energy of 1.5 MeV were selected as the source of ionizing radiation, and the samples were exposed to ions with a fluence of 10^{14}, $2 \cdot 10^{14}$, and 10^{15} cm^{-2}. In both types of diodes, a slight increase in the breakdown voltage was observed, as well as an increase in leakage current and a decrease in failure current with an increase in the TID. In the case of GGNMOS, the behavioral characteristic of secondary breakdown disappeared after irradiation, and a decrease in failure current was also observed. However, the paper did not provide explanations or reasons for this behavior of the devices after irradiation. The question also arises with regard to the influence of displacement damage defects on the behavior of samples during the ESD pulse, since irradiation with helium ions introduces a significant number of defects into the semiconductor volume.

In [7], the effect of gamma irradiation up to a TID of 200 krad on the characteristics of low-voltage and high-voltage dual-directional silicon controlled rectifiers (DDSCR) was investigated. Unlike the trigger voltage of low-voltage DDSCRs, the trigger voltage of high-voltage DDSCRs increased significantly with increasing TID. This is mainly due to an increase in breakdown voltage, and such rectifiers failed immediately after triggering. The increase in breakdown voltage after irradiation was associated with the accumulation of traps and interface traps (IT) in the field and gate oxides. This leads to an increase in the space charge region (SCR) of the *p-n* junctions, which determines the breakdown voltage. For the same reason, leakage currents increased after irradiation, leading to weak inversion of parasitic lateral transistors. This work made assumptions about the connection between changes in behavior during the ESD pulse of irradiated devices and the accumulation of traps and IT. Nevertheless, no quantitative comparison of the concentration of accumulated IT and changes in device parameters was performed.

The aim of the current work is to identify the mechanism of change in the resistance to ESD of high-power metal oxide semiconductor field effect transistors (MOSFETs) after gamma irradiation, as well as to study the relationship between the concentration of IT build-up during irradiation and the change in breakdown voltage under the influence of ESD (V_{ESD}). In order to calculate the concentration of IT, a method needs to be developed which will enable the volt-ampere (I–V) characteristic of the transistor to be directly linked to the concentration of IT.

1. PHYSICAL MECHANISM OF IT ACCUMULATION AND ITS IMPACT ON THE STABILITY OF HIGH-POWER MOSFETS TO ESD

Previously, the authors in [8] experimentally demonstrated that irradiation of high-power MOSFETs with gamma rays leads to improved resistance to ESD, with a higher breakdown voltage corresponding to higher TIDs. This effect was associated with the activation of a “parasitic” bipolar transistor in the structure of high-power MOSFETs under the influence of ESD. However,

under the influence of gamma irradiation, the gain of parasitic bipolar transistor (h_{21e}) degrades [9]. Thus, an increasingly higher ESD voltage is required to achieve the collector current value necessary for the secondary breakdown of the bipolar transistor and the subsequent failure of the MOSFET. The degradation of h_{21e} due to the effects of ionizing radiation occurs because of an increase in the recombination rate in the SCR emitter-base junction. This is manifested as an increase in base current at a fixed emitter bias. The recombination rate increases due to two interrelated effects: an increase in the surface recombination rate; and an expansion of the SCR emitter-base junction [10]. The increase in the surface recombination rate is proportional to the density of recombination centers at the Si/SiO_2 boundary of the emitter-base junction. Interface states, as one of the recombination centers, determine this increase in rate. However, the radiation-induced positive charge accumulated at the Si/SiO_2 boundary should also be taken into account due to the complex mechanism of their interaction. Surface states physically represent a Si atom with an unpassivated broken bond, formed after the Si–H bond was broken [11].

Today, it is believed that the dominant process in the mechanism of IT accumulation is proton hopping. In the first stage of this process, radiation-induced holes formed as a result of the generation of electron-hole pairs by ionizing radiation move through the oxide and free hydrogen in the form of protons under the action of an electric field. In the second stage, the protons move by hopping, and when they reach the Si/SiO_2 boundary, they react with the Si–H bond, forming H_2 and a trivalent Si defect [12, 13].

The current methods for measuring the gain of parasitic bipolar transistor (used for high-power MOSFETs with a short-circuited substrate terminal) involve heating the samples from 25 to 300°C and measuring the dependence of the drain current on the voltage at the drain of a closed transistor [14]. Such heating after irradiation changes the dynamics of IT accumulation [15, 16]. Therefore, h_{21e} changes during the measurement process, and the application of these methods in the current case will lead to unreliable results. In order to confirm the hypothesis that the resistance of high-power MOSFETs to ESD after gamma irradiation is determined by the accumulation of IT, the IT density of unirradiated samples needs to be calculated. The samples then need to be irradiated to several TID values, and the IT density calculated after irradiation. In each case the resistance to ESD needs to be investigated.

2. EXPERIMENT

Two types of high-power MOSFETs manufactured using HEXFET (hexagonal field-effect transistor) technology were selected as test samples. Therefore, thousands of parallel-connected MOSFET cells are placed in a single crystal, forming a hexagon: IRFR4615PbF (manufactured by International Rectifier, USA); and IRFR3710ZPbF (manufactured by Infineon Technologies, Germany). Before and after irradiation, drain-gate I–V curves were measured in the subthreshold region ($V_{g.s} < V_{th}$). From this the concentration of IT was calculated.

Gamma-ray irradiation with ^{60}Co was performed in threshold voltage measurement mode: $V_{g.s} = V_{d.s}$ and I_d = 100 μA for IRFR4615PbF and $V_{g.s} = V_{d.s}$ and I_d = 250 μA for IRFR3710ZPbF. IRFR4615PbF samples were irradiated to two TID values: 1.78 krad and 3.18 krad, IRFR3710ZPbF samples were irradiated to TID values of 2 krad and 3.9 krad. An ESD generator developed by the Research Institute of Scientific Instruments (RISI[1], Russia) was used as the ESD source. Its schematic diagram is shown in Fig. 1, and its main parameters are given in Table 1.

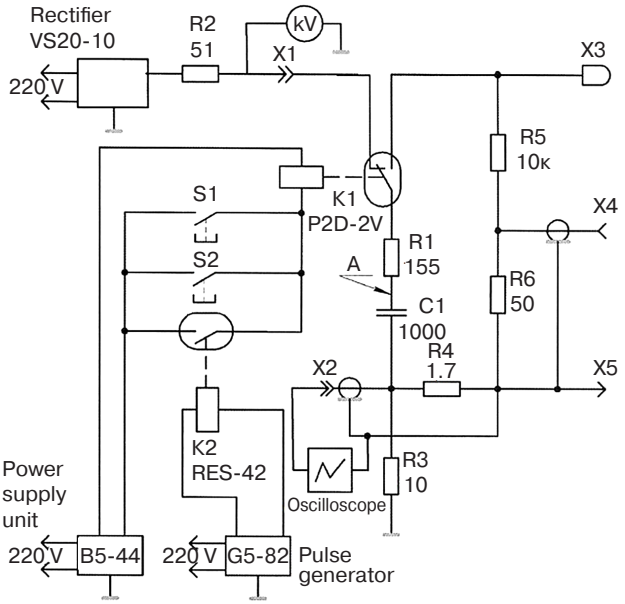

Fig. 1. Single-line diagram of the ESD generator[2]. S1 — "Start" pushbutton on the generator, S2 — remote control pushbutton for starting the generator, K1 — vacuum relay P2D-2V, K2 — intermediate relay RES-42, X1 — hook up of the high-voltage power source, X2 — current measuring connector, X3 — discharge tip, X4 — voltage measuring connector, X5 — reverse current conductor, C1 — discharge capacitor, R1 — discharge resistor, R2–R5 — resistors, B5-44 — power supply unit, G5-82 — pulse generator. The designations of the circuit elements correspond to those adopted in GOST 2.710-81[3]

[1] http://www.niipribor.ru/ (in Russ.). Accessed October 10, 2025.

[2] Figure 1 shows a diagram from the ESD generator passport.

[3] GOST 2.710-81. Interstate Standard. *Unified system for design documentation. Alpha-numerical designations in electrical diagrams*. Moscow: Izd. Standartov; 1985 (in Russ.).

Table 1. Basic parameters of the ESD generator

Parameter	Value
Output (test) continuously adjustable voltage, kV	From 1 to 20 ± 2
Output voltage polarity	Positive
Frequency of successive pulses, discharges per second	Up to 10
Peak value of discharge pulse current, A	Up to 100 ± 10
Duration of the current pulse front at the level of 0.1–0.9 amplitude, s	From $1 \cdot 10^{-9}$ to $1 \cdot 10^{-7}$
Stored energy in a storage capacitor C1, MJ	Up to 200 ± 10

The resistance of high-power MOSFET samples to ESD was determined by measuring the drain-gate I–V characteristic of the transistor after applying an ESD pulse to the drain (the source and gate are grounded at the moment of applying the pulse). The failure criterion was considered to be I–V behavior which is not typical for MOSFETs. The voltage range of the applied ESD pulse was 1–5 kV. If the sample withstood the test with one ESD pulse of the initial amplitude, the amplitude increased by 0.5 kV in the next applied pulse. The maximum withstand voltage when applying an ESD pulse (breakdown voltage value under ESD) was determined as the voltage value in the pulse after the appearance of I–V behavior not typical for MOSFETs.

3. METHOD FOR IT CONCENTRATION CALCULATION FROM SUBTHRESHOLD DRAIN-GATE CHARACTERISTICS

The subthreshold I–V characteristic is the drain-gate I–V characteristic in the weak inversion region. The surface potential in this case ranges within $\varphi_b \le \varphi_s \le 2\varphi_b$,

$$\varphi_b = \frac{kT}{q}\ln\left(\frac{N_a}{n_i}\right), \quad (1)$$

where q is the electron charge; k is the Boltzmann constant; T is the absolute temperature; N_a and n_i are the dopant concentration and the intrinsic concentration in the substrate, respectively.

In this case, the dependence of the drain current on the surface potential is described as follows [17]:

$$I_d = \frac{qDiWn_i^2}{\sqrt{2}L_{ch}N_a}\sqrt{\frac{\varepsilon_{Si}\varepsilon_0\varphi_T}{qN_a}}\left(\frac{\varphi_s}{\varphi_T}\right)^{-1/2}\exp\left(\frac{\varphi_s}{\varphi_T}\right), \quad (2)$$

wherein Di is the diffusion coefficient, L_{ch} is the channel length, W is the channel width, ε_{Si} is the permittivity of silicon, ε_0 is the electric constant, $\varphi_T = kT/q$.

If the source is connected to the substrate and grounded, then, by constructing a zone diagram (Fig. 2), $V_{g.s}$ can be expressed as the sum of the voltage drop across the oxide φ_{ox}, the voltage drop in silicon and the contact potential difference:

$$V_{g.s} = \varphi_s + \varphi_{ox} + \left[\frac{1}{q}\left(\chi_{Si} + \frac{E_g}{2}\right) + \varphi_b - \Phi_{me}\right], \quad (3)$$

wherein χ_{Si} is the electron affinity in silicon, E_g is the band gap, and Φ_{me} is the work function of the metal.

The voltage drop in the oxide can be estimated by knowing the distribution of the radiation-induced positive charge in the oxide ρ_{ox} and the electric field E_{ox} near the Si/SiO_2 boundary:

$$\varphi_{ox} = -E_{ox}d_{ox} - \frac{1}{\varepsilon_{ox}\varepsilon_0}\int_0^{d_{ox}}(d_{ox} - x)\rho_{ox}(x)dx, \quad (4)$$

wherein d_{ox} is the oxide thickness, ε_{ox} is the permittivity of SiO_2, x is the integration variable.

According to Gauss theorem for the electric displacement vector:

$$D_{ox} - D_{Si} = Q_{i.t}, \quad (5)$$

wherein D_{ox} is the electrical displacement in the oxide, D_{Si} is the electrical displacement in silicon, $Q_{i.t}$ is the IT charge.

In this case

$$\varepsilon_{ox}\varepsilon_0 E_{ox} - \varepsilon_{Si}\varepsilon_0 E_{Si} = Q_{i.t}. \quad (6)$$

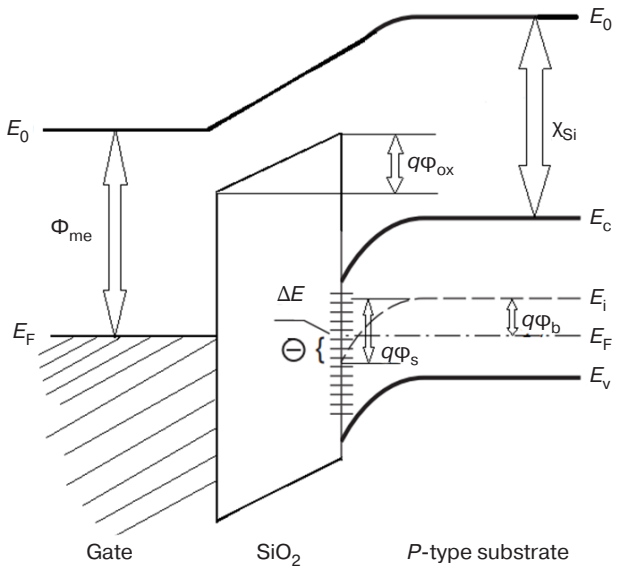

Fig. 2. Band diagram of a MOSFET structure with a *p*-type substrate: E_0 — vacuum level; E_F — Fermi level; E_v — energy corresponding to the top of the valence band; E_i — energy of the middle of the band gap; E_c — energy corresponding to the bottom of the conduction band, $\Delta E = q\Delta\varphi = q(\varphi_s - \varphi_b)$

As is known, in the upper part of the band gap ITs are acceptor-like (they can accept electrons), and in the lower part of the forbidden zone the states are donor-like (they can donate electrons [18]. ITs of the donor type are positively charged if they are located above the Fermi level and neutral if they are located below the Fermi level. ITs of the acceptor type are neutral if they are located above the Fermi level and negatively charged if they are located below the Fermi level. In the considered case of a *p*-type substrate in the weak inversion mode near the surface the Fermi level lies above the middle of the band gap, and only part of the acceptor levels in the energy range ΔE (Fig. 2).

The charged part of the levels can be expressed as follows:

$$\eta = \frac{\Delta E}{E_g}, \tag{7}$$

wherein ΔE is the distance from the middle of the band gap to the Fermi level near the Si/SiO_2 boundary.

In that case the IT is equal to:

$$Q_{i.t} = N_{i.t} q\eta = N_{i.t} q^2 \frac{\varphi_s - \varphi_b}{E_g}, \tag{8}$$

wherein $N_{i.t}$ is the IT concentration.

Applying (8) into (6), we obtain:

$$\varepsilon_{ox}\varepsilon_0 E_{ox} - \varepsilon_{Si}\varepsilon_0 E_{Si} = N_{i.t} q^2 \frac{\varphi_s - \varphi_b}{E_g}. \tag{9}$$

According to Poisson's equation:

$$\frac{d^2\varphi}{dx^2} = -\frac{\rho(x)}{\varepsilon_{Si}\varepsilon_0}, \tag{10}$$

wherein $\rho(x)$ is the total space charge density:

$$\rho(x) = q(-N_A + p(x) - n(x)), \tag{11}$$

$$p(x) = p_0 \exp\left(-\frac{\varphi(x)}{\varphi_T}\right), \tag{12}$$

$p(x)$ is the hole density distribution, p_0 is the initial hole concentration,

$$n(x) = n_0 \exp\left(-\frac{\varphi(x)}{\varphi_T}\right), \tag{13}$$

$n(x)$ is the electron density distribution, n_0 is the initial electron concentration.

Let us transform the left side of (10):

$$\frac{d^2\varphi}{dx^2} = \frac{d\frac{d\varphi}{dx}}{dx} = \frac{d\varphi}{dx}\cdot\frac{d\frac{d\varphi}{dx}}{d\varphi} = -E\frac{-d\mathrm{E}}{d\varphi} = E\frac{d\mathrm{E}}{d\varphi}. \tag{14}$$

Applying (14) into (10) and integrating over φ from φ_s to 0, we obtain:

$$\int_{E_{Si}}^{0} E\,dE = -\frac{q}{\varepsilon_{Si}\varepsilon_0}\int_{\varphi_s}^{0}\left[p_0\left(\exp\left(-\frac{\varphi_s}{\varphi_T}\right)-1\right) - n_0\exp\left(\frac{\varphi_s}{\varphi_T}\right)\right]d\varphi. \tag{15}$$

Taking into account that $p_0 = N_a$, and $n_0 = n_i^2 / N_a$, we obtain an expression for the field in silicon E_{Si}:

$$E_{Si} = \sqrt{\frac{2q\varphi_T N_a}{\varepsilon_{Si}\varepsilon_0}\left[\left(\frac{\varphi_s}{\varphi_T} + \exp\left(-\frac{\varphi_s}{\varphi_T}\right)-1\right) + \frac{n_i^2}{N_a^2}\left(\exp\left(\frac{\varphi_s}{\varphi_T}\right)-1\right)\right]}. \tag{16}$$

Thus, the system of equations (3, 4), (9), (16) directly connects the value $V_{g.s}$ with φ_s. By changing φ_s in the range φ_b from $2\varphi_b$ and using expressions (1)–(16), the dependences of I_d from $V_{g.s}$ can be numerically calculated for any values of the density of the accumulated radiation-induced charge and the concentration of the build-up ITs.

4. RESULTS AND ANALYSIS

Tables 2 and 3 present the results of calculating the concentration of IT and charge in the oxide (Q_{ox}) before and after irradiation, as well as the experimentally obtained values of the maximum voltage of the ESD pulse (V_{ESD}). The values of the breakdown voltage under ESD for non-irradiated samples were in the range of 3–4 kV for IRFR4615PbF and 4–4.5 kV for IRFR3710ZPbF.

Table 2 shows that for the IRFR4615PbF samples irradiated with a dose of 1.78 krad, ITs accumulated as a result of gamma irradiation were not built-up. Their concentration remained at the same level as before irradiation. For the samples irradiated with a dose of 3.9 krad, insignificant built-up IT already occurred, and the breakdown voltage under ESD exposure also remained virtually unchanged. For the IRFR3710ZPbF samples, the built-up ITs occurred at all values of the TID, and the concentration of the built-up ITs increased with an increase in the TID.

After irradiation, the breakdown voltage under ESD exposure increased. This is consistent with the proposed hypothesis that an increase in the concentration of built-up IT leads to degradation of the gain of the parasitic bipolar transistor. As a consequence, a higher ESD voltage is required for the collector current to reach the value necessary to initiate secondary breakdown of the bipolar transistor. It is worth noting that the initial concentration of IT in both types of samples is very high. This complicates the study, and even when irradiated to a TID close to the failure level, the number of built-up IT will be comparable to the initial concentration.

CONCLUSIONS

The study presents a theoretical description of the physical mechanism of the increase in breakdown voltage under the influence of ESD after gamma irradiation of high-power MOSFETs. The main reason for this phenomenon is the degradation of the gain of the parasitic bipolar transistor in the MOSFET structure, which, in turn, occurs due to the growth of the recombination rate in the SCR of the emitter-base junction, proportional to the density of the IT.

The resistance to ESD of two types of high-power MOSFETs was determined using a specially developed ESD generator before and after gamma irradiation. Gamma irradiation of the samples studied was carried out in the threshold voltage measurement mode on a ^{60}Co source at room temperature. Before and after irradiation, drain-gate I–V characteristics were recorded in the subthreshold region, from which the concentration of the IT was subsequently calculated. The study presents a method for calculating the dependence of the drain current on

Table 2. Experimental and calculated data for IRFR4615PbF

Sample No.	Absorbed dose, krad (Si)	Pre-irradiation		After irradiation		
		$N_{i.t}$, cm^{-2}	Q_{ox}, C	$N_{i.t}$, cm^{-2}	Q_{ox}, C	V_{ESD}, kV
1	1.78	$2.5 \cdot 10^{11}$	0	$2.5 \cdot 10^{11}$	$2.3 \cdot 10^{-8}$	2.5
2	1.78	$2.0 \cdot 10^{11}$	0	$2.0 \cdot 10^{11}$	$2.4 \cdot 10^{-8}$	3
3	3.18	$2.2 \cdot 10^{11}$	0	$2.4 \cdot 10^{11}$	$4.8 \cdot 10^{-8}$	3.5
4	3.18	$1.0 \cdot 10^{11}$	0	$1.2 \cdot 10^{11}$	$5.0 \cdot 10^{-8}$	2.5

Table 3. Experimental and calculated data for IRFR3710ZPbF

Sample No.	Absorbed dose, krad (Si)	Pre-irradiation		After irradiation		
		$N_{i.t}$, cm^{-2}	Q_{ox}, C	$N_{i.t}$, cm^{-2}	Q_{ox}, C	V_{ESD}, kV
1	2	$5.0 \cdot 10^{11}$	0	$8.0 \cdot 10^{11}$	$5.7 \cdot 10^{-8}$	5.5
2	3.9	$3.0 \cdot 10^{11}$	0	$7.0 \cdot 10^{11}$	$7.1 \cdot 10^{-8}$	5.5
3	3.9	$2.0 \cdot 10^{11}$	0	$6.0 \cdot 10^{11}$	$8 \cdot 10^{-8}$	5.5

the gate-source voltage for any values of the density of the accumulated radiation-induced charge and the concentration of built-up IT. The study also shows that with an increase in the concentration of built-up IT, the breakdown voltage of the sample under the influence of ESD increases.

Authors' contributions

D.M. Bakerenkova—hypothesis, development of a method for calculating the concentration of interface states, experimental studies, writing the text of the article.

A.S. Petrov—development of experimental methodology, validation, writing the text of the article, and editing.

REFERENCES

1. Paderov V.P., Silkin D.S., Goryachkin Yu.V., et al. Effect of proton irradiation on the breakdown voltage of a high-voltage *p–n* junction. *J. Commun. Technol. Electron*. 2017;62(6):616–620. https://doi.org/10.1134/S1064226917060158 [Original Russian Text: Paderov V.P., Silkin D.S., Goryachkin Yu.V., Khapugin A.A., Grishanin A.V. Effect of proton irradiation on the breakdown voltage of a high-voltage *p–n* junction. *Radiotekhnika i ehlektronika*. 2017;62(6):596–600 (in Russ.). https://www.elibrary.ru/ysugwj]
2. Shu L., Zhao Y.-F., Galloway K.F., Wang L., Wang X.-S., Yuan Z.-Y., Zhou X., Chen W.-P., Qiao M., Wang T.-Q. Effect of Drift Length on Shifts in 400-V SOI LDMOS Breakdown Voltage Due to TID. *IEEE Trans. Nucl. Sci*. 2020;67(11): 2392–2395. https://doi.org/10.1109/TNS.2020.2970743
3. Zhou X., Chen L., Chen C., Qiao M., Li Z., Zhang B. New Insight into Total-Ionizing-Dose Effect-Induced Breakdown Voltage Degradation for SOI LDMOS: Irradiation Charge Field Modulation. *IEEE Trans. Nucl. Sci*. 2023;70(4):659–666. https://doi.org/10.1109/TNS.2022.3231877
4. Seehra S.S., Slusark W.J. The Effect of Operating Conditions on the Radiation Resistance of VDMOS Power FETs. *IEEE Trans. Nucl. Sci*. 1982;29(6):1559–1563. https://doi.org/10.1109/TNS.1982.4336404
5. Blackburn D.L., Benedetto J.M., Galloway K.F. The Effect of Ionizing Radiation on the Breakdown Voltage of Power MOSFETS. *IEEE Trans. Nucl. Sci*. 1983;30(6):4116–4121. https://doi.org/10.1109/TNS.1983.4333092
6. Liang W., Alexandrou K., Klebanov M., Kuo C.-C., Kymissis I., Sundaram K.B., Liou J.J. Characterization of ESD protection devices under total ionizing dose irradiation. In: *IEEE 24th International Symposium on the Physical and Failure Analysis of Integrated Circuits* (*IPFA*), Chengdu, China: 2017. P. 1–4. https://doi.org/10.1109/IPFA.2017.8060225
7. Wu M., Lu W., Zhang C., Peng W., Zeng Y., Jin H., Xu J., Chen Z. The impact of radiation and temperature effects on dual-direction SCR devices for on-chip ESD protections. *Semicond. Sci. Technol*. 2020;35(4):045016. https://doi.org/10.1088/1361-6641/ab74ed
8. Arzamastseva D.M., Petrov A.S., Tapero K.I. Effect of Preliminary Gamma Irradiation on Degradation of Power *N*-MOS Transistors Influenced by Electrical Static Discharge. *Voprosy atomnoi nauki i tekhniki. Seriya: Fizika radiatsionnogo vozdeistviya na radioehlektronnuyu apparaturu*. 2023;3:19–22 (in Russ.).
9. Bakerenkov A.S., Felitsyn V.A., Chubunov P.A., Skorkin I.V. Temperature Dependence of Surface Recombination Current in Bipolar Transistors. In: *5th International Conference on Radiation Effects of Electronic Devices* (*ICREED*). Kunming, China: 2023. https://doi.org/10.1109/ICREED59404.2023.10390896
10. Kosier S.L., Schrimpf R.D., Nowlin R.N., Fleetwood D.M., DeLaus M., Pease R.L. Charge Separation for Bipolar Transistors. *IEEE Trans. Nucl. Sci*. 1993;40(6):1276–1285. https://doi.org/10.1109/23.273541
11. Lenahan P.M., Dressendorfer P.V. An Electron Spin Resonance Study of Radiation Induced Electrically Active Paramagnetic Centers at the Si/SiO_2 Interface. *J. Appl. Phys.* 1983;54(3):1457–1460. https://doi.org/10.1063/1.332171
12. McLean F.B. A Framework for Understanding Radiation-Induced Interface States in SiO_2 MOS Structures. *IEEE Trans. Nucl. Sci*. 1980;27(6):1651–1657. https://doi.org/10.1109/TNS.1980.4331084
13. Winokur P.S., McGarrity J.M., Boesch H.E. Dependence of Interface-State Buildup on Hole Generation and Transport in Irradiated MOS Capacitors. *IEEE Trans. Nucl. Sci*. 1976;23(6):1580–1585. https://doi.org/10.1109/TNS.1976.4328543
14. Reichert G., Raynaud C., Faynot O., Balestra F., Cristoloveanu S. Temperature dependence (300–600 K) of parasitic bipolar effects in SOI-MOSFETs. In: *Proceedings of the 7th European Solid-State Device Research Conference*. 1997.
15. Saks N.S., Dozier C.M., Brown D.B. Time Dependence of Interface Trap Formation in MOSFETs Following Pulsed Irradiation *IEEE Trans. Nucl. Sci*. 1988;35(6):1168–1177. https://doi.org/10.1109/23.25435
16. Winokur P.S., Boesch H.E., McGarrity J.M., McLean F.B. Field- and Time-Dependent Radiation Effects at the Si/SiO_2 Interface of Hardened MOS Capacitors. *IEEE Trans. Nucl. Sci*. 1977;24(6):2113–2118. https://doi.org/10.1109/TNS.1977.4329176
17. McWhorter P.J., Winokur P.S. Simple technique for separating the effects of interface traps and trapped-oxide charge in metal-oxide-semiconductor transistors. *Appl. Phys. Lett*. 1986;48(2):133–135. https://doi.org/10.1063/1.96974
18. Schwank J.R., Shaneyfelt M.R., Fleetwood D.M., Felix J.A., Dodd P.E., Paillet P., Ferlet-Cavrois V. Radiation Effects in MOS Oxides *IEEE Trans. Nucl. Sci*. 2008;55(4):1833–1853. https://doi.org/10.1109/TNS.2008.2001040

About the Authors

Diana M. Bakerenkova, Test Engineer, Research Institute of Scientific Instruments (8, Turaevo Industrial Area, Lytkarino, Moscow oblast, 140080 Russia). E-mail: arzamasceva.diana@mail.ru. RSCI SPIN-code 8543-8866, https://orcid.org/0009-0000-8670-812X

Aleksandr S. Petrov, Cand. Sci. (Eng.), Head of Department, Research Institute of Scientific Instruments (8, Turaevo Industrial Area, Lytkarino, Moscow oblast, 140080 Russia). E-mail: as_petrov@inbox.ru. Scopus Author ID 7401779679, RSCI SPIN-code 8304-5998, https://orcid.org/0009-0008-1198-980X

Об авторах

Бакеренкова Диана Максимовна, инженер-испытатель, Акционерное общество «Научно-исследовательский институт приборов» (140080, Россия, Московская обл., г. Лыткарино, промзона Тураево, стр. 8). E-mail: arzamasceva.diana@mail.ru. SPIN-код РИНЦ 8543-8866, https://orcid.org/0009-0000-8670-812X

Петров Александр Сергеевич, к.т.н., начальник отдела, Акционерное общество «Научно-исследовательский институт приборов» (140080, Россия, Московская обл., г. Лыткарино, промзона Тураево, стр. 8). E-mail: as_petrov@inbox.ru. Scopus Author ID 7401779679, SPIN-код РИНЦ 8304-5998, https://orcid.org/0009-0008-1198-980X

Translated from Russian into English by Lyudmila O. Bychkova
Edited for English language and spelling by Dr. David Mossop